

Influence of the patch field on work function measurements based on the secondary electron emission

N. Bundaleski,^{a)} J. Trigueiro, A. G. Silva, A. M. C. Moutinho, and O. M. N. D. Teodoro
Departamento de Física, CeFiTec, Faculdade de Ciências e Tecnologia, Universidade Nova de Lisboa, Campus de Caparica, P-2829-516 Caparica, Portugal

(Received 26 March 2013; accepted 26 April 2013; published online 14 May 2013)

A work function study based on the onset shift (i.e., following low energy cut-off) of secondary electron spectra has been used for the last four decades to monitor the deposition and adsorption in real time, measure the dipole momentum and polarizability of the surface layer, and determine the lateral distribution of the work function. In this work, we show that the onset shift depends on both the coverage of adsorbed species that change the work function and the size of low work function patches. Additionally, the extraction field, which is always applied in these measurements, may also influence the onset shift. Numerical calculations of the potential distributions above different non-uniform surfaces were performed in order to quantitatively determine each of these influences. Depending on the patch size, we define three measurement regimes in which the onset position is related to either the surface average of the work function (small patches), the minimum local work function (large patches), or a value in-between (intermediate size patches). Experimental data have corroborated these findings and demonstrated that manipulating the extraction field intensity enables transition between the measurement regimes. Typical misinterpretations due to neglecting the patch size contribution and the surface non-uniformity to the onset shift are analyzed. Additionally, possible application of work function study for determination of the growth mode in the case of submonolayer deposition was discussed. © 2013 AIP Publishing LLC. [<http://dx.doi.org/10.1063/1.4804663>]

I. INTRODUCTION

Work function study (WFS) based on the onset method is one of the common ways, known for almost 40 years, to measure a work function of conductive surfaces and follow its change.^{1,2} The technique is based on measuring the onset position (i.e., low energy cutoff) of the secondary electron energy distribution, which is related to the sample work function. Since the secondary electrons are usually produced by photon irradiation,^{3–16} the method is also known as photoemission measurement of the work function. However, WFS can also be performed by the use of any other beam that will provide secondary electron emission.^{17–24} Nowadays, these measurements are frequently realized using UV-light in order to provide absolute work function measurement, as it was initially proposed by Park and co-authors.⁶

WFS is typically used to follow adsorption and deposition processes in real time. The technique provides ultimate surface sensitivity and in some cases, such as the submonolayer adsorption of water on TiO₂ (110) rutile surface, it has a detection limit significantly below that of X-ray Photoelectron Spectroscopy (XPS),^{3–5,15} The principle of the onset method is based on the contact potential difference between the sample and the energy analyzer, implying that the potential energy just above the sample surface will differ from that along the equilibrium trajectory inside the energy analyzer. The energy levels of the sample and the analyzer in WFS measurements are presented in Fig. 1. The sample is

biased to a negative voltage U in order to assure that the electrons corresponding to the low energy cutoff will be registered. Then, the relation between the kinetic energy of electrons leaving the sample E and of that measured by the energy analyzer E' is

$$E' = E + \Phi - \Phi_A - eU = E + \Phi + E_0, \quad (1)$$

where e is electron charge, $E_0 = -\Phi_A - eU$, while Φ and Φ_A are work functions of the sample and the analyzer, respectively.²⁰ As the onset of the electron energy distribution corresponds to electrons emitted with zero kinetic energy, i.e., $E = 0$, its position in the energy spectrum will be at $\Phi + E_0$. Since the magnitude E_0 is constant, the onset shift directly corresponds to the change of the sample work function.

Surface deposition or adsorption of different species will alter the work function. The latter is usually quantitatively described by different models, such as that of Topping,²⁵ which relate the work function change with the surface coverage of the adsorbed/deposited species. This approach is applied assuming that the sample surface is uniform during the deposition/adsorption experiment. Although the latter is rarely the case, the Topping model is generally used without checking the surface uniformity and very often applied for coverage up to 1 monolayer (ML).^{11–16}

Having in mind obvious discrete nature of adsorbed species, surface uniformity can be achieved exclusively in idealized case of a sample surface without any defects and for coverage equal to zero or unity. Hence, the correspondence between the surface coverage and the onset shift should be generally considered starting from the assumption that the

^{a)} Author to whom correspondence should be addressed. Electronic mail: n.bundaleski@fct.unl.pt.

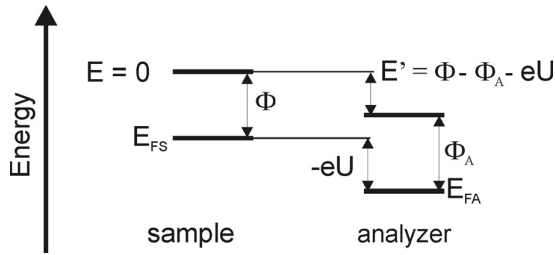


FIG. 1. Energy diagram of the sample and the analyzer in WFS measurements. E_{FS} and E_{FA} are the Fermi levels of the sample and the analyzer, respectively.

sample is non-uniform, i.e., each part of the sample surface has its own local work function. An excellent review on the concept of local work function and its measurement can be found in Ref. 26. The energy spectrum of secondary electrons emitted from a non-uniform surface is composed of different contributions, each corresponding to an emitting area with its own local work function. It is usually assumed the onset of each contribution is determined by its local work function.¹⁰ Consequently, the measured onset of the total energy spectrum will correspond to the areas with the lowest local work function.²⁰ Additionally, using a rastered probe (usually an electron beam) enables to determine the onset at the beam spot position. Applying the same interpretation, this onset will correspond to the local work function at the position of the beam spot. Surface mapping of the work function can then be achieved in this kind of measurements with a lateral resolution comparable to that of the primary beam diameter.^{17–22} Such experimental arrangement is known as Work Function Microscopy (WFM).

However, the assumption that the onset of each contribution corresponds to the local work function is also incorrect due to the so-called patch field effect.²⁷ Let us consider a surface consisting of two kinds of uniform patches having high (H) and low (L) local work functions Φ_H and Φ_L , respectively. A contact potential difference is established between these areas equal to $(\Phi_H - \Phi_L)/e$: Low work function areas will be positively biased with respect to those with high work function. Since all areas have the same Fermi level, the electrostatic potential will be higher in the proximity of L patches (i.e., potential energy for electrons will be lower) as opposed to H patches. Surface averaged work function of the sample will in this simplified case be $\langle\Phi\rangle = \eta \cdot \Phi_L + (1 - \eta) \cdot \Phi_H$, where η is the fraction of the sample surface covered by L regions. A potential energy distribution above two circular patches of L and H type having both $10\ \mu\text{m}$ in diameter is schematically presented in Fig. 2(a). Here we assume that $\Phi_L = 4\ \text{eV}$, $\Phi_H = 5\ \text{eV}$, and $\langle\Phi\rangle = 4.5\ \text{eV}$ (i.e., $\eta = 0.5$), whilst the Fermi level is taken as the reference. At distances from the surface very small compared to the patch diameter, the electron potential energy equals that of the local work function Φ_L or Φ_H . As the distance from the surface z is increased, the potential energy will be changing due to the field produced by surrounding patches, known as the patch field. Finally, far from the surface with respect to the patch dimensions, the electron potential energy becomes constant and equals $\langle\Phi\rangle$. The total energy spectrum of secondary electrons then consists

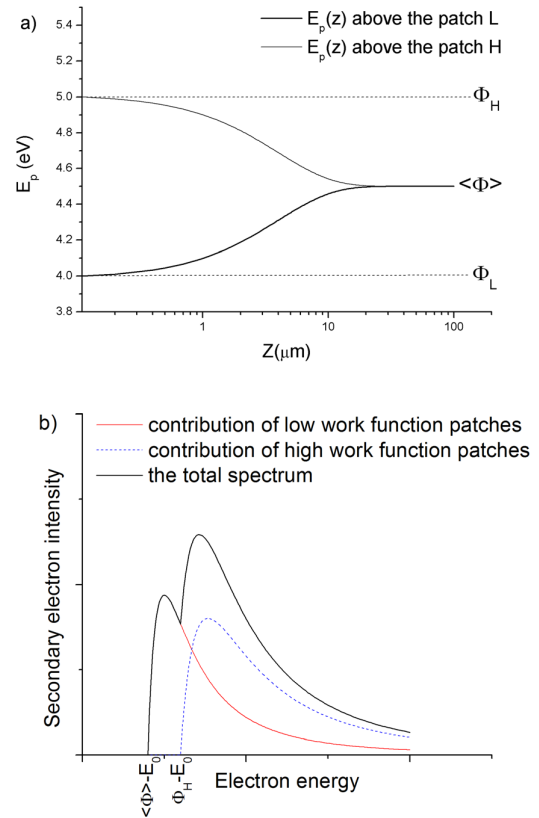


FIG. 2. (a) A scheme of the potential energy distribution in the absence of extraction field above two circular patches having local work functions $\Phi_L = 4\ \text{eV}$, $\Phi_H = 5\ \text{eV}$, each with diameter of $10\ \mu\text{m}$, and surface averaged work function $\langle\Phi\rangle = 4.5\ \text{eV}$; (b) a scheme of the secondary electron energy spectrum for this situation.

of two contributions, as can be seen from Fig. 2(b), with the onsets corresponding to $\langle\Phi\rangle$ and Φ_H . This conclusion is assumed to be generally valid for the electron emission from non-uniform surfaces:²⁷

The electrons emitted from areas with local work functions $\Phi_{loc} < \langle\Phi\rangle$ will have an additional energy barrier of height $\langle\Phi\rangle - \Phi_{loc}$, so that the height of the overall barrier for electron emission equals $\langle\Phi\rangle$.

The electrons emitted from regions with local work function $\Phi_{loc} > \langle\Phi\rangle$ are accelerated when leaving the surface, which will not affect the height of the energy barrier for electron emission.

Although known for a long time and studied in the case of the work function measurements using the diode method²⁸ and recently in the field emission experiments,²⁹ to the best of our knowledge, the effect of a patch field on the onset method has not yet been considered. Apparently, the problem is trivial: Since the electrons are detected far from the surface, the onset position should correspond to the surface averaged work function $\langle\Phi\rangle$ (cf. Fig. 2(b)). Another clear consequence of the patch field effect would be that WFM measurements cannot provide local work function mapping because the minimum observed local work function should actually correspond to $\langle\Phi\rangle$. This is, however, much more complicated issue since we still have to take into account the

modification of the energy barrier for the secondary electron emission due to the negative biasing of a sample with respect to the energy analyzer. The corresponding contribution to the electric field above the sample surface is here denoted as the extraction field.

The extraction electrostatic field will reduce the additional potential barrier of electrons emitted from low work function patches, just as in the case of the anomalous Schottky effect. This problem was recently studied by Binh and co-authors.²⁹ They performed a numerical calculations of the field distribution above the surface of a nanopatch-work cathode and showed that extraction field reduces the potential barrier for electron emission from low work function patches. If the field is strong enough, the potential barrier will become equal to the local work function. As it will be shown in this work, the extraction field intensity necessary to achieve this condition is inversely proportional to the patch dimensions. Consequently, the onset position will change with the dimension of low work function patches even if $\langle\Phi\rangle$ is kept constant. This effect may become very important during the deposition/adsorption since the size of islands will grow with coverage.

Clarifying ambiguities concerning the interpretation of WFS and WFM data and in particular understanding how the size of low work function patches influences the measurement is the main motivation behind this work. The potential distribution in the vicinity of a sample surface has been calculated for many patch configurations in order to establish general dependence of the energy barrier for electron emission on sample properties (patch size, coverage and $\langle\Phi\rangle$) and the extraction field intensity. Three different measurement regimes (attributed to small, intermediate, and large patches) are identified, as well as the corresponding patch diameter ranges as a function of the extraction field and the work function surface distribution. Additionally, it will be shown and experimentally confirmed that the intensity of the extraction field can be used to control the measurement regime. We shall discuss WFS and WFM experimental results from this perspective, highlight characteristic misinterpretations, and suggest convenient working parameters for these measurements. Finally, a possible application of WFS to determine thin film growth mode for submonolayer coverage will be considered.

II. CALCULATIONS OF THE POTENTIAL DISTRIBUTION ABOVE A NON-UNIFORM SURFACE

The patch field can be determined from the known work function distribution by solving the Laplace equation in the space above the sample. For the numerical solving of the Laplace equation we used the well-known program SIMION ver. 8.0, typically utilized for the simulation of charged particle optics. A non-uniform sample was modeled as a set of electrodes lying in the sample surface plane, each corresponding to a uniform area. The voltage between the electrodes corresponds to the contact potential difference. The exact electrode potentials were chosen to provide a mean surface potential of 0 V. The boundary of the space in which the potential is calculated is always kept at 0 V. The space volume was large enough to suppress the influence of the

boundaries on the potential distribution in the vicinity of the sample. Typical number of grid units in a volume in which the potential distribution has been calculated is 10^8 – 10^9 , depending on the volume symmetry. The convergence objective relative to the electrode voltage was 5×10^{-7} .

The first test involved a single circular patch of a diameter d deposited on a circular substrate with higher work function (cf. Fig. 3(a)). This case was used to estimate the accuracy of SIMION simulations since a similar configuration has an analytical solution. As it was shown in Ref. 30, the potential distribution along z axis of a conductive disc at potential V_0 located in an infinite plane at zero potential can be expressed as

$$V\left(\frac{z}{d}\right) = V_0 \cdot \left[1 - \frac{\frac{z}{d}}{\sqrt{\frac{1}{4} + \left(\frac{z}{d}\right)^2}} \right]. \quad (2)$$

In Fig. 3(b), we calculated the potential distribution normal to the surface $V(0, 0, z)$ above the patch, as well as $V(1.5d, 1.5d, z)$, i.e., above the substrate away from the patch. The contact potential difference was 1 V. The diameter of the sample was $5.7d$. Assuming a low work function patch with $d = 1$ mm, the grid unit was $7.3 \mu\text{m}$. In both cases, the potential changes from the local value $V(x, y, 0)$ (for short distances from the surface) and reaches a surface averaged

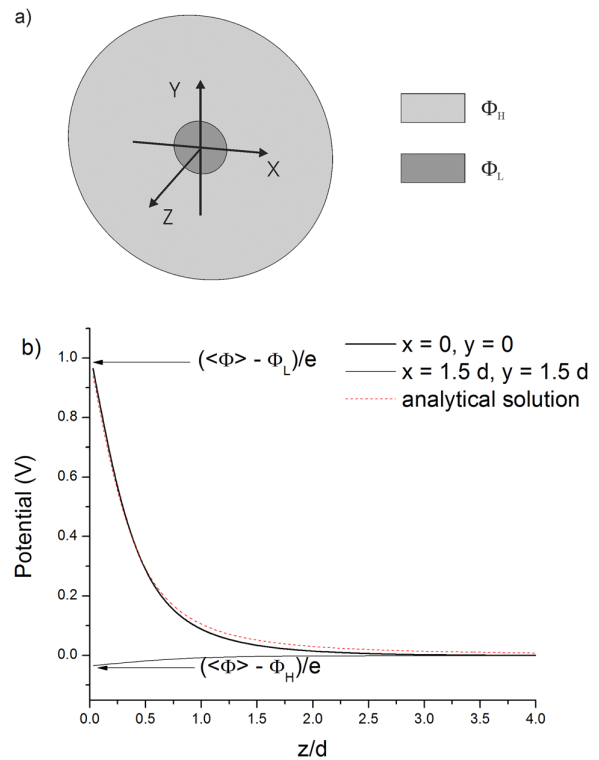


FIG. 3. Potential distribution atop a non-uniform surface consisting of a circular low work function patch of diameter d deposited on a circular substrate with a higher work function and a diameter equal to $5.7d$; (a) work function distribution; (b) potential distributions $V(0, 0, z)$ and $V(1.5d, 1.5d, z)$. The contact potential equals 1 V. The analytical solution for $V(0, 0, z)$ is based on Eq. (2).

potential $\langle V \rangle$ farther from the sample. The analytical dependence for $V(0, 0, z)$ based on Eq. (2) is also presented in Fig. 3(b). We can observe excellent match with the numerical result for $z/d \leq 0.75$. Although the numerical result reaches zero potential at shorter distance from the surface than the analytical one, the maximum discrepancy never reaches 0.05 V. This discrepancy is due to the finite size of the sample with respect to that of the patch. Indeed, when the sample diameter was increased to $50 d$, the discrepancy was much less than 1 mV. According to this comparison, we find the accuracy of SIMION simulations to be very good.

The numerically calculated potential distributions given in Fig. 3 can be very well fitted to exponential decay dependence. Consequently, taking the Fermi level as a reference, the potential energy distribution above a patch can be described as

$$E_p(x, y, z) = \langle \Phi \rangle - (\langle \Phi \rangle - \Phi_{\text{loc}}) \cdot e^{-\frac{z}{z_0}}, \quad (3)$$

where Φ_{loc} is the local work function at a point $(x, y, 0)$, and $\langle \Phi \rangle$ is the surface averaged work function. The expression (3) appears to be quite universal: It was also observed for a single square or rectangular patch, and even in the case of a surface with several uniformly distributed patches. This is not surprising since exponential function is a general analytical solution for $E_p(z)$ above the center of each patch in the case of an infinite 2D array of high and low work function rectangular patches forming a chessboard-like distribution.^{27,30}

In the case of a single patch situated in the center of a sample, the parameter z_0 is directly proportional to the square root of the patch area A if the fraction of area covered by low work function patches η is kept constant. The relation $z_0 \propto A^{1/2}$ is due to the nature of the Laplace equation. The consequence of this proportionality is illustrated in Fig. 2(a):

- At distances much shorter than $A^{1/2}$, the potential energy is equal to the local work function of the patch, Φ_{loc} ;
- While moving away from the surface the potential energy changes from Φ_{loc} towards $\langle \Phi \rangle$;
- At distances considerably longer than $A^{1/2}$, the potential energy equals $\langle \Phi \rangle$.

According to the results of many SIMION calculations that we performed, it appears that z_0 can be very well described as

$$z_0 = k(1 - \eta)\sqrt{A}. \quad (4)$$

Practically the same magnitude of the constant k is applicable for different patch shapes as long as the patches are not too elongated. For instance, the constant k is the same for square and circular patches, but decreases with the aspect ratio of rectangular patches. Numerous calculations have been performed for samples with several patches (both, circular and square), which showed general applicability of the expression (4). In these cases, the constant k depends weakly on the surface distribution of the work function, i.e., on the size and position of each patch: All values of z_0 obtained in these calculations can be described by Eq. (4), with $k = 0.48 \pm 0.03$.

As already stated in the Introduction, the extraction field due to biasing may significantly influence the potential

distribution above the surface. Let us consider a sample schematically presented in Fig. 3(a) with $\Phi_{\text{L}} = 4 \text{ eV}$ and $\Phi_{\text{H}} = 5 \text{ eV}$. An extraction field was introduced by biasing a circular extraction plate with a diameter of $14.4 d$ to a positive extraction voltage U_{ext} . The extraction plate was placed parallel to the sample at a distance of $5 d$. Since this geometry has cylindrical symmetry, the potential energy distribution can be conveniently presented in r - z plane (r is radial coordinate). The numerically calculated $E_p(r, z)$ for two different magnitudes of U_{ext} is presented in Fig. 4. It should be noted that the reference for the electron potential energy is Fermi level. This result clearly illustrates interplay between the patch field and the extraction field. For moderate extraction fields (Fig. 4(a)), electrons emitted from the low work function patch have to overcome an additional barrier. If the extraction field is sufficient, the height of the potential barrier becomes equal to the local work function (Fig. 4(b)).

It is clear from Fig. 4 that at a fixed height $z < d/2$ the potential energy distribution $E_p(r, z)$ has minimum at $r = 0$, and increases with r , i.e., with approaching the substrate. Apparently, the electrons emitted from a point on the low work function with $r > 0$ will have to overcome an “extra” potential barrier in order to reach the detector as compared

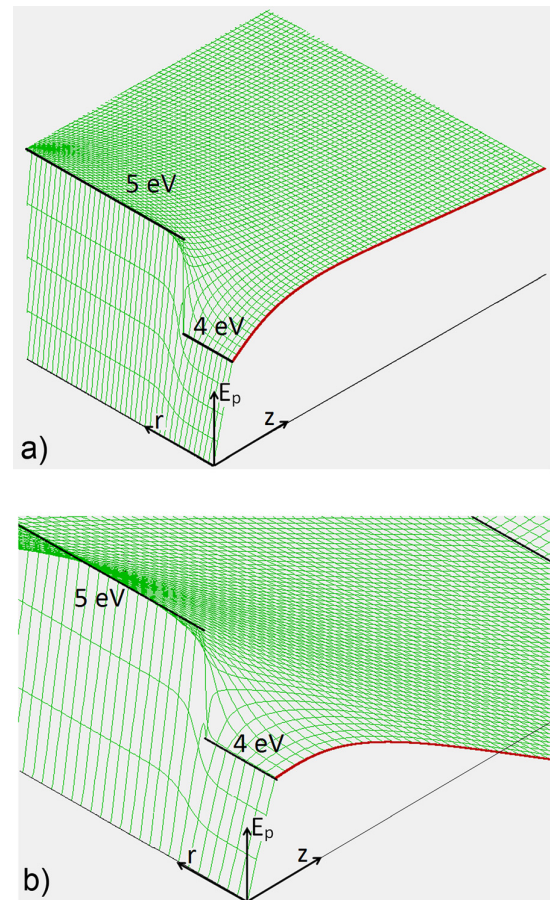


FIG. 4. Potential energy distribution $E_p(r, z)$ above the sample with work function distribution presented in Fig. 3(a) in the presence of extraction field: (a) $U_{\text{ext}} = 10 \text{ V}$; (b) $U_{\text{ext}} = 65 \text{ V}$. Patch and substrate work functions are 4 eV and 5 eV, respectively; the distance between the sample and the extraction plate of diameter $14.4 d$ is $5 d$.

to those emitted from the centre. While this should not influence the onset position in a WFS experiment, as it is determined by the lowest potential barrier, WFM results may be affected. However, the significance of this effect is not clear: The parallel component of the patch field will bend the trajectories towards the z -axis so that some of the electrons can bypass the “extra” potential barrier. In practice, it is very hard to quantitatively describe this effect because it strongly depends on the electron initial velocity and exact field distribution. Additionally, one should also have in mind that the step-like voltage distribution $V(z=0, r)$, implying infinite parallel component of the patch field at the interface is not physical. Therefore, true potential distribution has to be precisely calculated for proper evaluation of this effect. In the following discussions, we shall consider only the potential distribution along the z -axis.

In further analysis of the case treated in Fig. 4, we show in Fig. 5 numerically calculated $E_p(z)$ for different magnitudes of U_{ext} . The height of the potential barrier for electron emission from the low work function patch decreases with the extraction field intensity from $\langle\Phi\rangle = 4.98$ eV to Φ_L , whilst its position approaches the sample surface. Once potential barrier reaches Φ_L , further increase of the extraction voltage does not affect its height. In this example, the barrier height becomes equal to Φ_L for $U_{\text{ext}}^0 \approx 65$ V. Therefore, depending on the applied extraction field, WFS signal may correspond to the work function averaged over the surface, minimum local work function, or some value in-between. Similar result was also obtained in the simulations performed by Binh and co-authors.²⁹

WFS and WFM measurements are always performed in the presence of an extraction field. Therefore, estimating the energy barrier height for the electron emission from low work function patches under these conditions is of major interest. As the potential energy maximum position z_m is typically smaller than the patch diameter (cf. Fig. 5), the extraction field F in the vicinity of z_m can be considered approximately constant. Additionally, assuming that the potential energy decays exponentially with z in the absence of the extraction field (cf. Eq. (3)), the potential energy distribution along the axis of a patch with the local work function $\Phi_L < \langle\Phi\rangle$ is given by

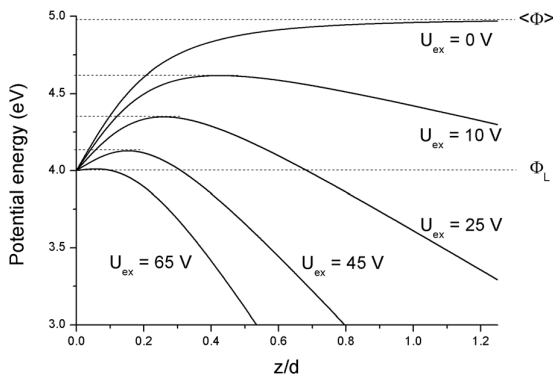


FIG. 5. Potential energy distribution along z -axis in the presence of extraction field for the case shown in Fig. 4. The energy barrier height for each extraction voltage is marked by the dashed lines.

$$E_p(z) = \langle\Phi\rangle - (\langle\Phi\rangle - \Phi_L) \cdot \exp\left(-\frac{z}{z_0}\right) - e \cdot F \cdot z. \quad (5)$$

The barrier maximum position z_m and height $E_{p\text{max}}$ can be then determined from the condition $dE_p/dz = 0$, which gives

$$z_m = z_0 \cdot \ln \frac{\langle\Phi\rangle - \Phi_L}{eFz_0} \quad (6)$$

and

$$E_{p\text{max}} = \langle\Phi\rangle - eFz_0 \left(1 + \ln \frac{\langle\Phi\rangle - \Phi_L}{eFz_0}\right). \quad (7)$$

Since z_m cannot be smaller than zero, these relations are valid only if $z_0 \leq (\langle\Phi\rangle - \Phi_L)/(e \cdot F)$. In order to compare the expression (7) with the result presented in Fig. 5, we are going to rearrange Eq. (7). For that purpose, let us define parameter $F_0 = (\langle\Phi\rangle - \Phi_L)/(e \cdot z_0)$, corresponding to the extraction field for which $E_{p\text{max}} = \Phi_L$. Further increase of the field will not change energy barrier unless the extraction field intensities characteristic for the Schottky effect (10^4 V/mm or more) are reached. Since the extraction field is scaled with the extraction voltage, we can write $F/F_0 = U_{\text{ext}}/U_{\text{ext}}^0$, where U_{ext}^0 is extraction voltage at which $E_{p\text{max}} = \Phi_L$. The expression (7) can be then rewritten as

$$E_{p\text{max}} = \langle\Phi\rangle - (\langle\Phi\rangle - \Phi_L) \cdot \frac{U_{\text{ext}}}{U_{\text{ext}}^0} \cdot \left[1 + \ln \frac{U_{\text{ext}}}{U_{\text{ext}}^0}\right], \quad (8)$$

$$0 < U_{\text{ext}} \leq U_{\text{ext}}^0.$$

The potential energy barrier vs. the extraction field obtained from the numerical result presented in Fig. 5 and using the analytical expression (8) is shown in Fig. 6. The surface averaged work function is in this case very close to Φ_H ($\langle\Phi\rangle = 4.98$ eV, $\Phi_H = 5$ eV). The analytical result is in very good agreement with the numerical calculations. The slight discrepancy is probably due to the non-uniformity of the extraction field in the vicinity of the sample surface and/or some discrepancy of the potential energy distribution

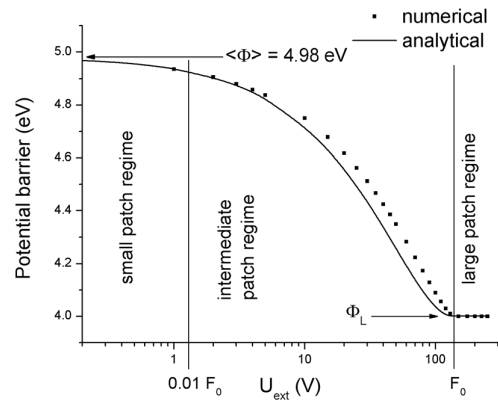


FIG. 6. Numerical and analytical calculation of the potential barrier for electrons emitted from a low work function patch vs. the extraction field. The numerical results are taken from the calculations shown in Fig. 5. Analytical results are based on Eq. (8), assuming that F_0 corresponds to $U_{\text{ext}}^0 = 65$ V.

from the expression (3). We see from Fig. 5 that as long as $F \leq 0.01 F_0$, $E_{pmax} \approx \langle \Phi \rangle$. For $F > 0.01 F_0$, the energy barrier is decreasing with the extraction field and reaches Φ_L for $F = F_0$.

According to the expression (7), the energy barrier E_{pmax} depends on the product of the extraction field F and the parameter z_0 . Since z_0 is directly proportional to the square root of the patch area (cf. Eq. (4)), E_{pmax} actually depends on the magnitude $F \cdot d$ in the case of a circular patch of a diameter d . The relative change of the extraction voltage (i.e., the extraction field) will then affect the energy barrier quantitatively in the same manner as the identical relative change of the patch diameter if F and $\langle \Phi \rangle$ (i.e., η) are kept constant. The equivalence between the relative changes of the extraction field and $A^{1/2}$ was also confirmed in our simulations for different arrangement and shapes of low work function patches. Therefore, low energy cut-off of the electron emission spectra corresponds to

- $\langle \Phi \rangle$ if the low work function patches are small,
- Φ_L when L patches are large enough, and
- a value in-between for the intermediate size of patches.

Consequently, we can define small, large and intermediate patch measurement regimes in WFS and WFM, depending on the typical patch size (cf. Fig. 6). For each regime, the onset shift has different meaning. It should be emphasized that the measurement regime depends also on both, η and the difference $\langle \Phi \rangle - \Phi_L$. Besides, it can be altered by changing the extraction field: The measurement is performed in a small patch regime if $F < 0.01 F_0$, whilst large patch regime will be achieved with extraction field $F \geq F_0$. WFS measurement regime might be also altered during a deposition/adsorption experiment due to the patch growth and consequent change of η and $\langle \Phi \rangle - \Phi_L$.

III. EXPERIMENTAL RESULTS

According to the study presented in Sec. II, change of the extraction field can alter the measurement regime in a WFS experiment. In order to experimentally test this influence, a special sample was prepared. In the middle of a mechanically polished $10 \times 10 \text{ mm}^2$ polycrystalline nickel sheet (Goodfellow, thickness of 0.1 mm, 99% purity), a hole with a diameter of 1.6 mm was drilled. The sheet was then pressed onto a 1 mm thick indium plate (Goodfellow, 99.999% purity). Due to the softness of indium a nickel surface with a circular In patch in the middle was obtained, which practically corresponds to the hypothetical sample schematically presented in Fig. 3(a). Work functions of these metals should be about $\Phi_{Ni} \approx 5.2 \text{ eV}$ and $\Phi_{In} \approx 4.1 \text{ eV}$ (Ref. 31). For this geometry, the work function of the patch should equal Φ_{In} while the surface averaged work function is approximately Φ_{Ni} . The idea of the experiment was to follow the onset shift of electrons emitted exclusively from the In patch as a function of the sample biasing voltage U . We stress that the negative biasing voltage in the experiment is equivalent to U_{ext} from Sec. II. As long as the measurements are performed in the small or large patch measurement regimes (corresponding to low and high biasing voltages,

respectively), the onset of the secondary electron distribution should follow the biasing voltage according to Eq. (1). For very low U the onset should correspond to Φ_{Ni} and for high U to Φ_{In} . In the intermediate patch regime, i.e., for intermediate biasing voltages, an additional onset shift will appear that will depend on $-U$, i.e., U_{ext} in a way described by Eq. (8).

We assume in the experiment that In and Ni surfaces are uniform in terms of work function. Strictly speaking, this is not the case: Both surfaces are polycrystalline, while Ni surface has also modest initial purity. The typical dimension of these non-uniformities is in micrometer range, just as the expected corresponding values of z_0 . Assuming that the contact potential difference between different non-uniformities is of the order of 1 V, the extraction field necessary for their observation in a large patch regime is at least $F_0 \approx 10^3 \text{ V/mm}$. As it was shown in Sec. II, measurement of Ni and In surfaces will be performed in the small patch regime if the extraction field is below $0.01 \cdot F_0$, i.e., 10 V/mm (cf. Fig. 6). Consequently, as long as the extraction field is below 10 V/mm we should consider Φ_{Ni} and Φ_{In} as surface averaged work functions of the nickel substrate and the indium patch, respectively. On the other hand, the extraction field necessary to observe the indium patch in the large patch regime is $F_0 \approx (\Phi_{Ni} - \Phi_{In}) / (e \cdot 0.48 \cdot A^{1/2}) = 1.65 \text{ V/mm}$ (A is the In patch area). Since this field is not enough to resolve non-uniformity of Ni and In surfaces, both, the substrate and the patch, can be considered uniform.

The experiment has been performed in the multipurpose surface analysis system³² with a base pressure in the low 10^{-10} mbar range, which provides analysis using standard techniques such as XPS or Low Energy Ion Scattering (LEIS). The secondary electron energy spectra were taken using VSW Class 100 system for energy analysis, which consists of the hemispherical electrostatic energy analyzer and transfer charged particle optics. The measurements were performed in the fixed analyzer transmission mode with pass energy of 10 eV. The collected secondary electrons were emitted normal to the sample surface. The resolution was about 1%. The onset was determined as the intersection of extrapolated steepest slope of the low energy part of the spectrum with the energy axis. The sample was initially sputter cleaned with 3 keV Ar^+ beam and then the secondary electron distribution was measured for various biasing voltages U . Electron emission was obtained by 4 keV Ar^+ ion bombardment of the sample with the incident angle of 45° . The ion beam diameter is about 0.3 mm.

Preliminary measurements have been performed on a clean single crystal Ag(100) surface in order to test the influence of the extraction field on the onset position. For the biasing voltage in the range from 10 eV to 500 eV the onset was following U according to Eq. (1) with the standard deviation of 0.08 eV, which we consider as experimental error. This result is a confirmation that the charged particle optics does not contribute to noticeable onset shift due to sample biasing. The position of the ion beam (i.e., the position from which the electrons are emitted) has been checked by LEIS performed by the same Ar^+ beam used to produce secondary electron emission. The presence of the corresponding single

scattering peak and its intensity was used to control from which area the electrons were emitted, i.e., from the indium patch or the nickel substrate.

The onset position vs. $-U$ in the case of the primary beam focused on In patch and Ni surface after the subtraction of the biasing voltage is presented in Fig. 7. Zero of the onset scale corresponds to the mean onset position for Ni. For the Ni surface, the onset shift follows the biasing voltage according to Eq. (1) in the frame of the experimental error. This confirms our estimation that the intensity of the extraction field was not enough to resolve the non-uniformity of the Ni surface. When electrons are emitted from the In patch, the onset shifts additionally with the biasing voltage towards lower work functions for about 1 eV and saturates for $U_0 = -125$ V. If this saturation is interpreted as the entrance into the large patch regime, U_0 corresponds to the parameter $F_0 \approx 1.65$ V/mm. The electric field distribution inside the chamber is hard to estimate. However, since the distance between the sample surface and entrance into the analyzer system is about 70 mm, the interpretation according to which $U_0 = -125$ V corresponds to the extraction field of 1.65 V/mm is reasonable. While the transition between the intermediate and the large patch regime is evident in Fig. 7, this is not the case for the transition between the small and the intermediate patch regime. The latter should take place at about $U \approx -1.25$ eV, which is out of the range of the biasing voltage applied in the experiment: We were not able to perform reliable WFS measurements for $-U < 5$ V.

Once U_0 is determined, we can calculate the onset shift as a function of the biasing voltage using Eq. (8). For that purpose the ratio $U_{\text{ext}}/U_{\text{ext}}^0$ is replaced by U/U_0 , whilst the difference $\langle\Phi\rangle - \Phi_L$ is assumed to be equal to $\Phi_{\text{Ni}} - \Phi_{\text{In}} = 1.1$ eV. The calculated dependence of the onset shift on the biasing voltage agrees very well with the experimental result, as can be seen from Fig. 7. Small discrepancies between the calculation and the experiment may be related to the surface cleanliness and roughness, which could

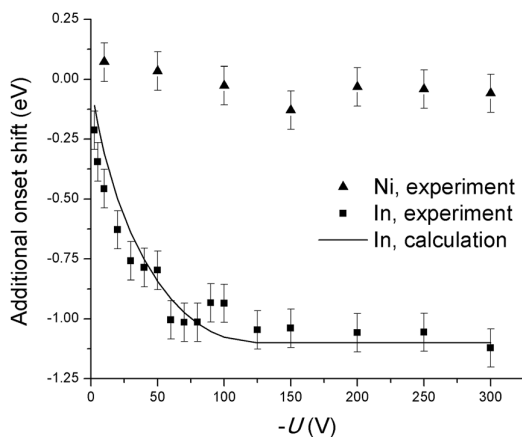


FIG. 7. Additional onset shift vs. the biasing voltage obtained from the energy spectrum of secondary electrons emitted from a 1.6 mm In patch and a Ni substrate. Zero of the onset scale corresponds to the mean onset position of spectra recorded from Ni. The experimental error is estimated as ± 0.08 eV (see the text). The calculation is based on Eq. (8) for $U_0 = -125$ V, $\Phi = \Phi_{\text{In}}$ and $\langle\Phi\rangle = \Phi_{\text{Ni}}$.

influence Φ_{Ni} and Φ_{In} , but also to the possible non-uniformity of the extraction field close to the sample surface. Nevertheless, we find this agreement as a clear proof that the extraction field indeed has influence on the onset position and can alter the measurement regime.

IV. DISCUSSION

Interpretation of WFS experimental data appears to be much more complex than usually thought as it is not possible to establish a general correlation between the onset shift and the amount of adsorbed or deposited species that change the sample work function. The origin of the problem is in the surface non-uniformity: The latter is achieved only in the case of an ideal surface without any defects and for coverage equal to zero or unity. The onset is always related to the work function averaged over some area, the size of which depends on the extraction field, and the overall surface distribution of the work function. In the further analysis we shall mainly consider ideal, uniform substrate with the concentration of adsorption sites equal to n . Then, for coverage below a monolayer, two different situations can occur:¹

1. The adsorbed/deposited species is distributed in a random and diluted way; to further simplify this case, we assume uniform distribution of these species, so that their local coverage θ_{loc} equals the surface averaged one, i.e., $\theta_{\text{loc}} = \langle\theta\rangle$.
2. The adsorbed/deposited species forms uniform 2D islands which already possess the internal order of the completed monolayer. Therefore, the surface consists of two kinds of uniform patches, i.e., those for which θ_{loc} equals unity (2D islands), or zero (the substrate). If these species decrease the work function, $\eta = \langle\theta\rangle$; otherwise, $\eta = 1 - \langle\theta\rangle$.

Unless the extraction field is extremely high, the onset will always correspond to $\langle\Phi\rangle$ in case 1. In case 2, the onset may correspond to the surface averaged work function of a sample $\langle\Phi\rangle$, local work function of low work function patches Φ_L , or to a magnitude in-between the two. This will depend on the measurement regime, i.e., on the size of low work function patches, the biasing voltage, the fraction of the surface covered by low work function patches η , and $\langle\Phi\rangle - \Phi_L$. We shall now discuss different WFS experiments in the light of the proposed interpretation.

A. Measurement of the dipole moment and the polarizability

Submonolayer surface adsorption can cause dipole formation. Depending on their orientation, these dipoles can partially cancel or enhance the original dipole layer made by electrons that spill-out the surface. Change of the work function will depend on the concentration of dipoles, their dipole moment, and polarizability. The Topping model²⁵ is typically applied to correlate the onset shift and the coverage of adsorbed species.^{11–16} In most of the cases, the composition measurement is performed by a technique providing only averaged surface composition. Assuming all adsorbed species lie in the same layer (no 3D growth), $\langle\theta\rangle$ can be obtained from these measurements. Then, onset shift ΔS (considered

to be equal to the work function change $\Delta\Phi$) is correlated to $\langle\theta\rangle$ as

$$\Delta S = \Delta\Phi = -\frac{e}{\epsilon_0} \mu \cdot n \cdot \frac{\langle\theta\rangle}{1 + \kappa\alpha(n\langle\theta\rangle)^{3/2}}, \quad (9)$$

where μ is the dipole moment at very small local coverage, α is polarizability of dipoles, and κ is a constant related to the arrangement of adsorbed/deposited species at the surface. The dipole moment and the polarizability are determined by fitting the onset shift vs. surface concentration of adsorbed species. Applying the model in this way is correct only when the surface remains uniform during the experiment (case 1). A good test of surface uniformity is the time evolution of the secondary electron energy spectrum: If the energy spectrum just shifts along energy axis without changing the shape, the surface probably keeps uniformity during the adsorption/deposition experiment.²⁸ Since this is usually not the case, the interpretation of the onset shift should depend on the measurement regime.

In the *small patch regime*, the onset shift will correspond to the change of the surface averaged work function $\Delta\langle\Phi\rangle$. When applying the Topping model correctly

$$\Delta S = \Delta\langle\Phi\rangle = -\frac{e}{\epsilon_0} \mu \cdot n \cdot \left\langle \frac{\theta_{\text{loc}}}{1 + \kappa\alpha(n\theta_{\text{loc}})^{3/2}} \right\rangle, \quad (10)$$

where the bracket denotes surface averaging. If the surface is kept uniform during the experiment (case 1), this equation becomes identical to Eq. (9). On the other hand, if uniform islands are formed (case 2), $\Delta\langle\Phi\rangle$ is mainly due to the patch growth, i.e., change of η , since $\theta_{\text{loc}} = 1$ inside a patch. This case will be discussed further in Sec. IV C. The expected dependence $\Delta S(\langle\theta\rangle)$ for these two cases is schematically presented in Fig. 8.

Let us also consider briefly a situation which does not correspond to either of the two cases: The adsorbed species do not form 2D islands, although they are distributed in a non-uniform way. If the local coverage θ_{loc} is low, the depolarization factor $\kappa\alpha(n\theta_{\text{loc}})^{3/2}$ can be neglected. Then, the

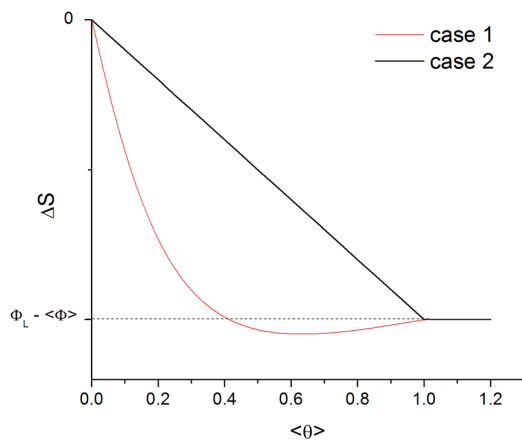


FIG. 8. A scheme of the onset shift vs. $\langle\theta\rangle$ taken in the small patch regime when the adsorbed/deposited species is diluted and uniformly distributed (case 1) or form 2D islands with $\theta_{\text{loc}} = 1$ (case 2).

onset shift can be approximated to $-e \cdot n \cdot \mu \cdot \langle\theta\rangle/\epsilon_0$, i.e., the slope of the onset shift vs. $n \cdot \langle\theta\rangle$ will be then proportional to the dipole moment (cf. Fig. 8, case 1). We emphasize that Eqs. (9) and (10) become identical after neglecting the depolarization factor. Therefore, the standard way of applying Topping model may give correct values for μ , but certainly not for α since this approach will fail for coverage at which depolarization factor is considerable (Eqs. (9) and (10) are becoming different).

In the *large patch regime*, the onset shift corresponds to the difference between the local work functions of the low work function patches Φ_L and the substrate. In the framework of the Topping model,

$$\Delta S = \Delta\Phi_L = -\frac{e}{\epsilon_0} \cdot \frac{n \cdot \mu \cdot \theta_L}{1 + \kappa \cdot \alpha \cdot (n \cdot \theta_L)^{3/2}}, \quad (11)$$

where θ_L is the local coverage inside the low work function patch. For uniform surfaces (case 1) $\theta_L = \langle\theta\rangle$, i.e., expression (11) is identical to Eq. (9). When two kinds of uniform patches are created (case 2), we may differ two situations: (a) if low work function patches correspond to the 2D islands of adsorbed species $\theta_L = 1$; and (b) when low work function patches correspond to the substrate $\theta_L = 0$, i.e., $\Delta\Phi_L = 0$ eV. In any case, the onset shift will not depend on the surface composition and therefore, μ and α cannot be determined.

The consequences of inappropriate application of the Topping or an equivalent model will strongly depend on the analyzed system, the experimental setup and, in particular, on the regime in which the measurement is performed. The standard approach based on Eq. (9) is typically applied in straightforward manner without checking the surface uniformity, and even when it is known that adsorbed species form 2D islands. Deposition of alkali atoms on a clean metal surface is an example in which the assumption of uniform surfaces could be accepted due to the repelling of dipoles and the high surface mobility of adsorbed alkali atoms. The expression (9) was utilized by many authors to determine the dipole moment and the depolarization of adsorbed species (cf. Ref. 33 and references therein). This approach provides satisfactory values for the dipole moment, determined from the slope of $\Delta\Phi$ vs. $\langle\theta\rangle$ dependence at low coverage, but fails in determining the polarizability. Introducing more complicated models to describe the experimental results did not yield in satisfactory results as well. The problem in some systems can be due to the surface non-uniformity, as in the case of potassium adsorption on Ru(1010):²⁸ As we already discussed, if the dipoles do not form 2D islands but are still not uniformly distributed, only μ could be correctly determined.

B. Work function microscopy

Another example in which misinterpretation of the onset shift is encountered is WFM, as it was already mentioned in the Introduction. Conventional WFM measurements performed by Scanning Auger Microscope (SAM) are apparently tempting since it is possible to perform both work function and composition mapping at the same time. The

surface regions with the local work function $\Phi_{\text{loc}} > \langle \Phi \rangle$ will be indeed observed with a lateral resolution determined by the beam spot size. However, in the case of patches with $\Phi_{\text{loc}} < \langle \Phi \rangle$, the onset will correspond to a value in the interval $[\Phi_{\text{loc}}, \langle \Phi \rangle]$ depending on the biasing voltage, the work function surface distribution and the difference $\langle \Phi \rangle - \Phi_{\text{loc}}$. (In some cases, depending on the work function surface distribution, the onset for low work function patches may even correspond to a value greater than $\langle \Phi \rangle$.) This problem is particularly significant due to a low biasing voltage typically used in these measurements.²²

Working in the large patch regime is mandatory for correct work function mapping. Therefore, in order to provide high lateral resolution, it would be necessary to perform measurements with strong extraction fields. This approach would make realization of WFM in a SAM system very complicated due to the influence of the field on the trajectories of primary electrons, although not impossible.¹⁷ Much more convenient is to use UV or X-ray photons as a probe. This kind of measurements, known as Energy Filtered Photoelectron Emission Microscopy (EF-PEEM), is actually performed (see Refs. 34 and 35, for instance). The extraction field applied in this technique is typically in the range of 10^4 V/mm. Assuming the difference $\langle \Phi \rangle - \Phi_{\text{loc}}$ is about 1 eV, from the value of the parameter F_0 we can estimate the resolution for work function mapping to about $0.1 \mu\text{m}$ if η is small (cf. Eq. (4)). However, since z_0 decreases with η , comparatively large patches might not be always observed in the large patch regime. Moreover, strictly speaking, for $\eta \approx 1$ the measurements will be performed in the small patch regime although, in this particular case, we already have that $\langle \Phi \rangle \approx \Phi_{\text{L}}$. A simple way to test the regime in which EF-PEEM measurements are performed would be to check if onset shift follows the change of the biasing voltage according to Eq. (1).

C. Thin film deposition

One of the typical applications of WFS with low biasing voltage is to follow the sub-monolayer thin film growth.^{7,8,11–16,23,33} According to the generally accepted theory, at the initial phase of deposition (i.e., for very low coverage) the atoms arriving from the gas phase diffuse along the surface until they meet another adatom or a very small cluster, giving rise to nucleation of islands. At this stage, the number of nucleation centers will increase roughly linearly with the increase of coverage. When the concentration of nucleation centers becomes comparable to that of adatoms and small clusters, the probability of an adatom to contribute to a formation of a new nucleation center is similar to the probability that it joins already formed stable clusters. Therefore, the adatoms will contribute to both formation of nuclei and growth of already present stable clusters. With further increase of the concentration of stable clusters, the deposition of adatoms will contribute exclusively to the island growth. Later on, at coverage as high as 0.6 ML, a coalescence of growing clusters takes place.³⁶

From this general picture, we can draw few conclusions concerning the work function change during the

submonolayer growth in the framework of the Topping model. First of all, a surface cannot be considered uniform during a typical thin film deposition experiment. Then, the local concentration of deposited species in an island is constant so that the local work function of the island is constant during the deposition (cf. Eq. (10)). Therefore, it is not possible to extract any information concerning μ and α of deposited species by following work function change in this kind of experiment.

Depending on the thin film growth mode, 2D or 3D islands will be formed on a surface. It has been confirmed for many systems that deposition atop of an existing island practically does not change the local work function (for instance, cf. Refs. 11, 12, 15, 23, 33, 37, and 38). Strictly speaking, surface roughness may also alter Φ_{loc} (Ref. 26), but the effect on the onset should not be significant (see below). Starting from this assumption we may conclude that the onset shift in a WFS experiment is mainly due to the change of the sample coverage, i.e., growth of both cluster density and their lateral size. Can the ultimate surface sensitivity of WFS be used to yield information concerning the thin film growth process? The answer to this question may be positive if WFS is performed in the small patch regime during the deposition.

Let us consider an experiment in which deposition is followed by WFS using low biasing voltage ($F \approx 0.25$ V/mm, which is typical in our case): The onset shift is measured *in situ* as a function of the fluence of deposited species. We assume that for any fluence all deposited islands have approximately equal size. Assuming the local coverage of an island equals unity, the surface averaged coverage $\langle \theta \rangle$ is equal to the fraction of surface covered with a deposit. If islands with local work function Φ_{I} grow on uniform substrate with a work function Φ_0 , $\langle \Phi \rangle = (1 - \langle \theta \rangle) \cdot \Phi_0 + \langle \theta \rangle \cdot \Phi_{\text{I}}$. In further analysis, we treat separately two characteristic situations: A deposited material may decrease or increase work function of a sample.

When the deposited species decrease the sample work function, the onset of the electron emission spectrum is due to the emission from the deposited islands. According to Eqs. (4) and (7), the onset shift is in this case given as

$$\Delta E_{p\text{max}}(\langle \theta \rangle) = -\langle \theta \rangle \cdot \Delta \Phi - eFk\sqrt{A} \cdot (1 - \langle \theta \rangle) \cdot \left[1 + \ln \frac{\Delta \Phi}{eFk\sqrt{A}} \right], \quad (12)$$

where $\Delta \Phi = \Phi_0 - \Phi_{\text{I}}$. Initially, for small $\langle \theta \rangle$, the islands are very small (i.e., $F \ll \Delta \Phi / (ekA^{1/2})$) and the measurement is performed in the small patch regime: $\Delta E_{p\text{max}} \approx -\langle \theta \rangle \cdot \Delta \Phi$. The second term of Eq. (12) corresponds to the difference between the onset measured in the small patch regime, and the intermediate or large patch regime. This difference is negligible for coverage $\langle \theta \rangle \approx 1$, when we can expect formation of larger low work function patches due to the coalescence. The second term may have some significance only if patches of area above 0.1 nm^2 are formed at $\langle \theta \rangle$ well below 1, which is not likely. Therefore, we may say that the observed onset shift can be considered directly proportional to $\langle \theta \rangle$ in most of the cases.

If deposited material increases the work function, the onset will now be related to the electron emission from the substrate. The onset shift can be described by Eq. (12) if we replace $\langle\theta\rangle$ by $1 - \langle\theta\rangle$, and having in mind that A is now size of substrate areas not covered by the deposit. Besides, $\Delta\Phi$ will be now negative. Assuming uniform distribution of deposit islands on the uniform substrate, this case appears to be equivalent to the previous one with reversed time. For low coverage the measurement may be performed in the large or intermediate patch regime, but the discrepancy from a result obtained in the small patch regime should not be significant. At higher $\langle\theta\rangle$, the substrate areas become small and the measurement will be done in the small patch regime. Besides, if the substrate has microscopic or even smaller non-uniformities, which should be a typical situation, the measurement is essentially done in the small patch regime during the whole experiment.

Assuming that WFS experiments during the thin film growth are performed in the small patch regime, the onset shift should be directly proportional to $\langle\theta\rangle$. We show in Fig. 9 a qualitative dependence of the onset shift vs. the amount of deposited material J for different growth modes. In the case of a pure 2D growth $\langle\theta\rangle \propto J$, so that the onset shift will be directly proportional to J (cf. Fig. 8, case 2). If the islands grow in 3D, the coverage (and therefore the onset shift) is not going to be directly proportional to J . For some systems, a quasi-2D growth takes place: The islands initially grow as 2D clusters but at a critical coverage a 2D/3D transition occurs. The fluence at which critical coverage takes place is the one at which $\Delta S(J)$ dependence is no longer linear.

Deposition of the first-row transition 3d metals (Ti-Cu) on the atomically clean Mo(110) surface at room temperature is considered as a 2D island growth.³⁷ Work function change measured by the retarding field method, which should give very similar results as the onset method, is for these systems directly proportional to the coverage up to 0.5–0.8 ML, and reaches saturation at about 1 ML. Having in mind the error in coverage estimation of about 15%–20% in these measurements, this result supports the proposed model of the onset shift during the deposition.

Besides the 3D growth, non-linear $\Delta S(J)$ dependence can be also due to a non-uniform substrate. The onset shift is proportional to a local work function change at the

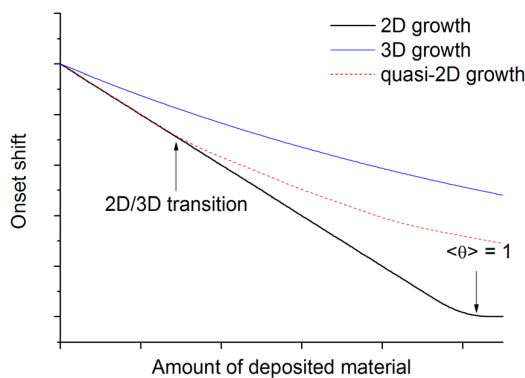


FIG. 9. A scheme of expected onset shift measured during a thin film deposition for different growth modes.

adsorption site $\Delta\langle\Phi\rangle = -\langle\theta\rangle \cdot \delta\Phi_{\text{loc}}$. Islands may preferentially grow at some specific sites, such as different kinds of defects. Then, when these sites are occupied, the nucleation will take place on other substrate sites. Therefore, in this case, it could happen that $\delta\Phi_{\text{loc}}$ is changing during the deposition which will be observed as non-linear $\Delta S(J)$ dependence. Another cause of the onset shift can be change of surface roughness during the deposition due to the Smoluchowski effect.³⁹ The consequence of this effect on $\langle\Phi\rangle$ is typically in the range 0.01–0.02 eV (cf. Ref. 26), which is well below the typical overall onset shift during the deposition. Finally, in some specific cases, such as deposition of some alkaline^{7,12,15,33} or alkaline earth metals,³⁸ the assumption that the local coverage is constant during the exposure does not hold. For these systems local coverage increases with the amount of deposited material, which contributes to the enhanced depolarization. Hence, at higher exposures the work function increases before reaching saturation at full coverage.

V. CONCLUSION

WFS is a simple yet highly sensitive experimental technique which may reveal important information about surface modification, including its exposure to fluxes of various atoms and molecules. However, its potentials are reduced in many cases due to the limited agreement with different theoretical findings. While the applicability of different models is usually questioned, we show here that the problem may also be related to data misinterpretation. In an attempt to partially overcome the experimental problems, we propose some general guidelines for performing WFS.

A first step in any work function study is to determine whether the surface may be considered uniform during the experiment, by monitoring the time evolution of the secondary electron energy spectrum shape. If yes, any model may be directly applied to the data. If not, the next step consists in determining the measurement regime by testing whether onset shift follows the biasing voltage in a way described by Eq. (1).

In vast majority of cases low biasing voltage is applied, and WFS measurement is most probably performed in the small patch regime for which the onset corresponds to the surface averaged work function $\langle\Phi\rangle$. Dipole moment of adsorbed/deposited species can be determined from the slope of the work function change vs. $n \cdot \langle\theta\rangle$ only if the local coverage inside a low work function patch θ_{loc} is initially small. Polarizability can be determined if θ_{loc} is also measured, assuming that the local coverage is changing during the exposure.

In the large patch regime, minimum work function is monitored and a model can be applied only if θ_{loc} is measured. Working in it is necessary to provide work function mapping. EF-PEEM is particularly suitable experimental technique for this purpose. However, one should be careful with the data analysis due to the paradox that increase of the patch size may provoke transition from the large patch to intermediate patch measurement regime.

WFS in the small patch regime appears to be especially interesting for monitoring thin film growth because of the

typically constant local coverage in the deposited islands. The onset shift is then directly proportional to $\langle \theta \rangle$ and therefore enables to identify different growth modes (i.e., 2D, 3D, and quasi-2D growth). In the case of an ideally uniform substrate, WFS is expected to be much more sensitive to growth modes than other surface analysis techniques due to its ultimate surface sensitivity. Apart from the possibility to provide valuable information on the growth process, this kind of WFS measurements may be of interest in calibration of quartz crystal microbalance thickness monitor. However, other effects, such as substrate non-uniformity and surface roughness, might reduce applicability of WFS in determining thin film growth modes. Therefore, more work is needed to reveal its true potentials for this application.

ACKNOWLEDGMENTS

We thank Dr. Alexander Tolstoguzov from Universidade Nova de Lisboa for many discussions that helped in clearing out some ideas presented in this work. This work was supported by Fundação para a Ciência e Tecnologia do Ministério da Ciência, Tecnologia e Ensino Superior (FCT/MCTES), under Contract PTDC/FIS/100448/2008 and the Portuguese Research Grant Pest-OE/FIS/UI0068/2011 through FCT-MEC. João Trigueiro also acknowledges FCT/MEC for his PhD scholarship.

¹H. Lüth, *Surfaces and Interfaces of Solids* (Springer-Verlag, Berlin, 1993).

²S. Evans, *Chem. Phys. Lett.* **23**, 134 (1973).

³J.-M. Pan, B. L. Maschhoff, U. Diebold, and T. E. Madey, *J. Vac. Sci. Technol. A* **10**, 2470 (1992).

⁴H. P. Marques, A. R. Canário, A. M. C. Moutinho, and O. M. N. D. Teodoro, *Appl. Surf. Sci.* **255**, 7389 (2009).

⁵A. G. Silva, N. Bundaleski, A. M. C. Moutinho, and O. M. N. D. Teodoro, *Appl. Surf. Sci.* **258**, 2006 (2012).

⁶Y. Park, V. Choong, Y. Gao, B. R. Hsieh, and C. W. Tang, *Appl. Phys. Lett.* **68**, 2699 (1996).

⁷J. L. LaRue, J. D. White, N. H. Nahler, Z. Liu, Y. Sun, P. A. Pianetta, D. J. Auerbach, and A. M. Wodtke, *J. Chem. Phys.* **129**, 024709 (2008).

⁸W. Song and M. Yoshitake, *Appl. Surf. Sci.* **251**, 14 (2005).

⁹G. Zha, W. Jie, X. Bai, T. Wang, L. Fu, W. Zhang, J. Zhu, and F. Xu, *J. Appl. Phys.* **106**, 053714 (2009).

¹⁰N. D. Orf, I. D. Baikie, O. Shapira, and Y. Fink, *Appl. Phys. Lett.* **94**, 113504 (2009).

¹¹M. Pivetta, F. Patthey, W. D. Schneider, and B. Delley, *Phys. Rev. B* **65**, 045417 (2002).

¹²K. Ozawa and K. Edamoto, *Surf. Sci.* **524**, 78 (2003).

¹³K. Onda, H. Li, and H. Petek, *Phys. Rev. B* **70**, 045415 (2004).

¹⁴H. Fukagawa, H. Yamane, S. Kera, K. K. Okudaira, and N. Ueno, *Phys. Rev. B* **73**, 041302(R) (2006).

¹⁵Y. Sun, Z. Liu, and P. Pianetta, *J. Vac. Sci. Technol. A* **25**, 1351 (2007).

¹⁶H. Fukagawa, S. Hosoumi, H. Yamane, S. Kera, and N. Ueno, *Phys. Rev. B* **83**, 085304 (2011).

¹⁷G. Eng and H. K. A. Kan, *Appl. Surf. Sci.* **8**, 81 (1981).

¹⁸G. Bachmann, W. Berthold, and H. Oechsner, *Thin Solid Films* **174**, 149 (1989).

¹⁹G. Bachmann, H. Oechsner, and J. Scholtes, *Fresenius' Z. Anal. Chem.* **329**, 195 (1987).

²⁰H. Oechsner, *Fresenius' Z. Anal. Chem.* **355**, 419 (1996).

²¹O. M. N. D. Teodoro and A. M. C. Moutinho, *Key Eng. Mater.* **230–232**, 165 (2002).

²²A. Imanishi, E. Tsuji, and Y. Nakato, *J. Phys. Chem. C* **111**, 2128 (2007).

²³H. P. Marques, A. R. Canário, A. M. C. Moutinho, and O. M. N. D. Teodoro, *Vacuum* **82**, 1425 (2008).

²⁴H. Nonaka, T. Shimizu, K. Arai, A. Kurokawa, and S. Ichimura, *J. Surf. Anal.* **9**, 344 (2002).

²⁵J. Topping, *Proc. R. Soc. London, Ser. A* **114**, 67 (1927).

²⁶K. Wandelt, *Appl. Surf. Sci.* **111**, 1 (1997).

²⁷C. Herring and M. H. Nichols, *Rev. Mod. Phys.* **21**, 185 (1949).

²⁸S. Surnev and M. Kiskinova, *Appl. Phys. A* **46**, 323 (1988).

²⁹V. T. Binh, R. Mouton, Ch. Adessi, V. Semet, M. Cahay, and S. Fairchild, *J. Appl. Phys.* **108**, 044311 (2010).

³⁰J. D. Jackson, *Classical Electrodynamics* (John Wiley & Sons, New York, 1962).

³¹*Handbook of Chemistry and Physics*, 84th ed., edited by D. R. Lide (CRC Press LLC, 2004).

³²O. M. N. D. Teodoro, J. M. A. C. Silva, and A. M. C. Moutinho, *Vacuum* **46**, 1205 (1995).

³³R. W. Verhoef and M. Asscher, *Surf. Sci.* **391**, 11 (1997).

³⁴L. F. Zagonel, M. Bäurer, A. Bailly, O. Renault, M. Hoffmann, S. J. Shih, D. Cockayne, and N. Barrett, *J. Phys.: Condens. Matter* **21**, 314013 (2009).

³⁵O. Renault, B. Brochier, A. Roule, P.-H. Haumesser, B. Kromker, and D. Funnemann, *Surf. Interface Anal.* **38**, 375 (2006).

³⁶T. T. Magloev, K. Christmann, P. Lecante, and A. M. C. Moutinho, *J. Phys.: Condens. Matter* **14**, L273 (2002).

³⁷U. V. Slooten, W. R. Koppers, A. Bot, H. M. V. Pinxteren, A. M. C. Moutinho, J. W. M. Frenken, and A. W. Kleyn, *J. Phys.: Condens. Matter* **5**, 5411 (1993).

³⁸H. Brune, *Surf. Sci. Rep.* **31**, 125 (1998).

³⁹R. Smoluchowski, *Phys. Rev.* **60**, 661 (1941).